RESEARCH ARTICLE

# Proteomic profiling of tandem affinity purified 14-3-3 protein complexes in *Arabidopsis thaliana*

*Ing-Feng Chang[1,2,3]*,**, Amy Curran[1]*, Rebekah Woolsey[4], David Quilici[4], John C. Cushman[1], Ron Mittler[1], Alice Harmon[5] and Jeffrey F. Harper[1]**

[1] Department of Biochemistry and Molecular Biology, University of Nevada, Reno, NV, USA
[2] Institute of Plant Biology, National Taiwan University, Taipei, Taiwan
[3] Department of Life Science, National Taiwan University, Taipei, Taiwan
[4] Proteomic Core Facility, University of Nevada, Reno, Reno, NV, USA
[5] Department of Botany and the Genetics Institute, University of Florida, FL, USA

Received: May 25, 2008
Revised: January 31, 2009
Accepted: February 14, 2009

In eukaryotes, 14-3-3 dimers regulate hundreds of functionally diverse proteins (clients), typically in phosphorylation-dependent interactions. To uncover new clients, 14-3-3 omega (At1g78300) from Arabidopsis was engineered with a ''tandem affinity purification'' tag and expressed in transgenic plants. Purified complexes were analyzed by tandem MS. Results indicate that 14-3-3 omega can dimerize with at least 10 of the 12 14-3-3 isoforms expressed in Arabidopsis. The identification here of 121 putative clients provides support for *in vivo* 14-3-3 interactions with a diverse array of proteins, including those involved in: (i) Ion transport, such as a $K^+$ channel (GORK), a $Cl^-$ channel (CLCg), $Ca^{2+}$ channels belonging to the glutamate receptor family (1.2, 2.1, 2.9, 3.4, 3.7); (ii) hormone signaling, such as ACC synthase (isoforms ACS-6, -7 and -8 involved in ethylene synthesis) and the brassinolide receptors BRI1 and BAK1; (iii) transcription, such as 7 WRKY family transcription factors; (iv) metabolism, such as phosphoenol pyruvate carboxylase; and (v) lipid signaling, such as phospholipase D (β and γ). More than 80% (101) of these putative clients represent previously unidentified 14-3-3 interactors. These results raise the number of putative 14-3-3 clients identified in plants to over 300.

**Keywords:**
14-3-3 / Arabidopsis / Interactome / Kinase / Tandem affinity purification

## 1 Introduction

In eukaryotes, 14-3-3 proteins regulate diverse cellular functions through hundreds of different protein–protein interactions (clients). In the yeast *Saccharomyces cerevisiae*, a double knockout of its 14-3-3 genes (*BMH1 and BMH2*) is lethal, indicating that some 14-3-3 interactions are essential. 14-3-3s are encoded by multi-gene families in animals (*e.g.* seven isoforms in mammals) and plants. In Arabidopsis, mRNA expression has been detected for 12 of the 15 14-3-3 genes (GF14/phi, GF14/chi, GF14/omega, GF14/psi, GF14/upsilon, GF14/lamda, GF14/nu, GF14/kappa, GF14/mu, GF14/epsilon, GF14/omicron, GF14/iota) [1]. Eleven of these 12 isoforms have been detected in a proteomic analysis [2]. Unique structural features associated with each isoform are expected to provide differences in sub-cellular localization, client-specific interactions and differences in regulation by phosphorylation or cation binding [3]. Because 14-3-3s can heterodimerize, the 12 expressed Arabidopsis

**Correspondence:** Dr. Jeffrey Harper, Department of Biochemistry and Molecular Biology, University of Nevada, Reno, Reno, NV 89557, USA
**E-mail:** jfharper@unr.edu
**Fax:** +1-775-784-1286

**Abbreviations: ACC,** 1-aminocyclopropane-1-carboxylate; **BB,** binding buffer; **CDPK,** calcium-dependent protein kinase-1; **FDR,** false-positive identification rate; **GFP,** green fluorescence protein; **GLR,** glutamate receptor family; **MudPIT,** multiple dimensional protein identification technology; **PA,** phosphatidic acid; **PEP,** phosphoenol pyruvate; **RT,** room temperature; **SCX,** strong cation-exchange; **TAP,** tandem affinity purification; **TEV,** tobacco etch viruse; **Y2H,** yeast two-hybrid

*These authors contributed equally to this work.
**Additional correspondence: Dr. Ing-Feng Chang, E-mail: ifchang@ntu.edu.tw

isoforms can potentially form 78 different dimers, each with a unique combination of potential regulatory features.

Most 14-3-3 client interactions are thought to be promoted by phosphorylation of a target-binding site on the client. The target-binding sites include Mode-1 (K/R xx $S_p/T_p$ x P) and Mode-2 (K/R xxx $S_p/T_p$ x P) (where x represents any amino acid and the $S_p/T_p$ is phosphorylated) [4, 5]. A third motif, Mode-3 ($YT_pV$), was found in $H^+$-ATPase [6]. Other non-consensus sites have also been discovered, some of which do not require phosphorylation [7].

The two major challenges to understanding the biological functions of 14-3-3s are (i) the need to first identify the plethora of potential clients, and (ii) on an individual basis, determine how the client's structural or enzymatic functions are altered. Many 14-3-3 interactions have been shown to regulate the client protein directly. For example, in plants, one of the best-studied examples is the 14-3-3 activation of the plasma membrane $H^+$-ATPase [6]. However, 14-3-3s can also regulate cellular functions by bringing together two different clients [8]. This mode of action is possible because 14-3-3s dimerize, and each 14-3-3 subunit has its own binding cleft. As the list of 14-3-3 clients grows, so does the number of unique combinations of clients potentially brought into the same complex as a result of a 14-3-3 scaffold.

Hundreds of potential 14-3-3 clients have now been identified in fungal, plant and animals systems. Several proteome-wide survey approaches have been used, including classic yeast two-hybrid (Y2H) searches, *in vitro* binding of cell extracts to a 14-3-3 affinity column, and co-purification of *in vivo* complexes formed with epitope-tagged 14-3-3s. For example, in animal systems, the purification of *in vivo* complexes formed with epitope-tagged 14-3-3 has contributed to the identification of more than 300 potential 14-3-3 clients [9–11]. Although each experimental strategy has its *pros* and *cons*, one advantage of purifying epitope-tagged 14-3-3 complexes is that the identification of a potential client is accompanied by evidence supporting an *in vivo* interaction. One of the disadvantages of the Y2H approach is that some 14-3-3 complexes will never be recovered; for example, in cases where the yeast is missing a kinase activity required for phosphorylation of a particular plant client. Although *S. cerevisiae* has around 119 kinases, it does not have representatives for the more than 600 receptor kinases present in plants [12].

To date, most of the potential 14-3-3 clients from plants have been obtained by Y2H and *in vitro* binding studies [13]. To complement these approaches, we performed a MS-based proteomic analysis of tandem affinity purification (TAP)-tag affinity purified 14-3-3 complexes. For this purpose, we engineered a stable transgenic Arabidopsis plant expressing a tandem affinity-tagged 14-3-3 omega. Our TAP-tag contained a standard protein-A motif, but was modified to replace the calmodulin-binding site with a 6x. His motif to avoid the co-purification of complexes associated with calmodulin-binding proteins. After purifying TAP-tagged 14-3-3 complexes, in parallel with a control TAP-tagged green fluorescence protein (GFP), the co-purifying proteins were subjected to in-solution protease digestion followed by MALDI TOF-based multiple dimensional protein identification technology (MudPIT) analysis. We identified 131 proteins that specifically co-purified with the TAP-tagged 14-3-3, including 10 14-3-3 isoforms and 121 putative clients. Of these, 101 represent new potential 14-3-3 clients that have not previously been identified. For example, our results support a role of 14-3-3 in regulating new clients involved in the transport of $Ca^{2+}$, $K^+$ and $Cl^-$, enzymes involved in ethylene biosynthesis, brassinolide signal transduction, and WRKY transcription factors to name a few. This analysis brings the total number of potential 14-3-3 clients in plants to more than 300. This makes 14-3-3s one of the most connected nodes of interaction on the emerging protein–protein interaction map of the plant proteome.

## 2 Materials and methods

### 2.1 Transgenic plant lines and growth conditions

*Arabidopsis thaliana* cv Columbia plants were transformed with 35s::GFP-TAP2 (ps346, plant line ss687 and ss820) or 35s::14-3-3 omega-YFP-TAP2 (ps472, plant line TL3169) through an *Agrobacterium* (GV3101)-mediated floral dip transformation method [14]. Transgenic plants were selected on plates consisting of 1/2x MS salts (Sigma), 0.5 g/L MES, pH 5.7, and 25 ug/mL hygromycin B (Invitrogen) or 50 ug/mL kanamycin (Sigma), respectively. Seedlings were then transferred after 10–14 days to 200 mL liquid media consisting of 1/2x MS salts, 0.5g/L MES, pH 5.7, and 2% sucrose and grown for 6–7 wk under low light conditions with continuous shaking at room temperature (RT).

### 2.2 Constructs and cloning

#### 2.2.1 Recombinant tobacco etch virus (TEV) protease

GST-TSPN-S2 (ps308) encodes a mutant version of TEV protease with reduced auto-cleavage activity [15]. It was constructed as a sandwich fusion between GST at the N-terminus and a Strep Tag (S2) at the C-terminus in a modified pGEX-4T vector (Pharmacia), which harbors an ampicillin resistance marker (see Supporting Information Fig. 1 for plasmid sequence).

#### 2.2.2 Plant constructs

35s::GFP-TAP2 (ps346) encodes an N-terminal GFP fused to Protein-A, a TEV protease cleavage site and a 6xHis, under the control of the cauliflower mosaic virus 35s promoter

 

(Fig. 1A). The parent plant transformation vector was pGreenII, providing hygromycin resistance in plants and kanamycin resistance in bacteria [16] (see Supporting Information Fig. 2 for plasmid sequence). 35s::14-3-3 omega-YFP-TAP2 (ps472) encodes an N-terminal 14-3-3 omega (At1g78300) fused to a YFP, the same affinity tag used in 35s::GFP-TAP2, and expressed under the control of a 35s promoter (Fig. 1A). The parent plant transformation vector was pBIN, providing kanamycin resistances in plants and bacteria, [17] (see Supporting Information Fig. 3 for plasmid sequence).

### 2.3 Purification of GST-tagged TEV protease

Overnight cultures of *Escherichia coli* harboring GST-TSPN-S2 (ps308) in 2XYT media +200 μg/mL ampicillin were diluted tenfold, grown for 1 h at 30°C, and expression of

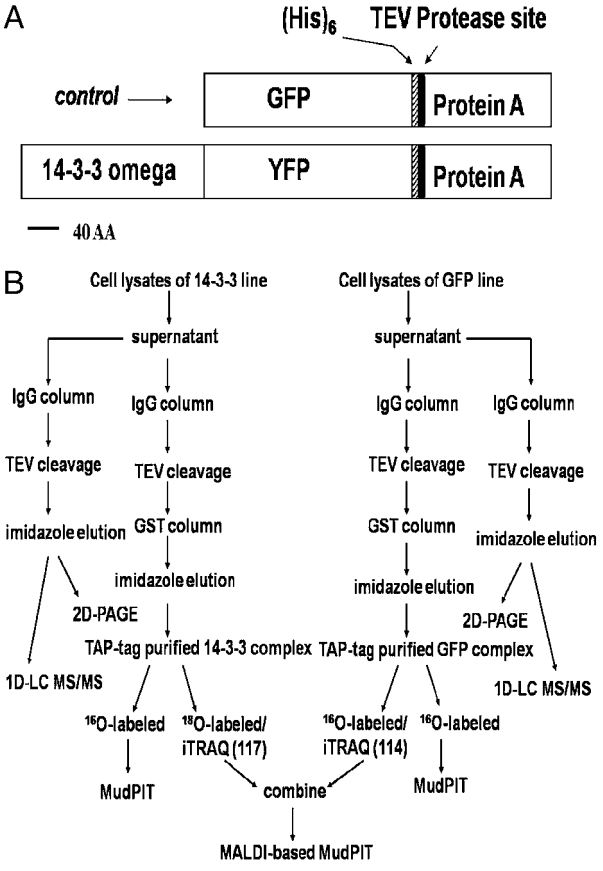


**Figure 1.** Flow chart of MS-based proteomic analysis of TAP-tag affinity purified 14-3-3 protein complex. (A) Diagram showing domain organization of GFP-TAP2 (control) and 14-3-3 omega-YFP-TAP2 (bait) fusion proteins. (B) Soluble (supernatant) proteins were separated from membranes and organelles by ultracentrifugation and processed as shown. Purified samples were subjected to either MALDI-based or ESI-based MudPIT analysis. Quantitative analysis was conducted using $^{16}O/^{18}O$ and iTRAQ labeling methods followed by MudPIT analyses.

GST-TSPN-S2 induced by addition of 0.5mM IPTG. Cells were grown three more hours at 30°C. Cells were harvested, and the cell pellet resuspended in 20 mL GST-binding buffer (BB; 20 mM Tris-HCl, pH 8.5, 10 mM EDTA, 100 mM NaCl) +1 mM PMSF and 1 mg/mL lysozyme. After incubation on ice for 10–30 min, the mixture was frozen at −70°C until used. The sample was thawed quickly, and Triton X-100 added to 0.4% v/v. Cells were broken by sonication for 6 min at 4°C. Cell debris was pelleted at 10 000 × *g* for 10 min. The supernatant was mixed with 400 μL of a 50% slurry of glutathione agarose (Sigma) pre-washed with 3 × 5 mL GST-BB and incubated for 1 h at 4°C. The glutathione agarose beads were pelleted at 200–300 × *g* for 30 s, washed with 3 × 10 mL GST-BB, and transferred to a biospin column (Bio-Rad). TSPN fusion protein was eluted with 2 × 500 μL GST-elution buffer (100 mM Tris-HCl, pH 8.5, 500 mM NaCl, 0.1 mM EDTA, 10mM glutathione) and concentrated in a centricon (YM-30, Millipore). Glycerol was added to a final concentration of 50%. Aliquots were frozen and stored at −70°C. The concentration of TSPN was determined *via* the Bradford method [18], and greater than 90% purity verified by SDS-PAGE (10% polyacrylamide gel) and staining with CBB [18].

### 2.4 TAP-tag affinity purifications

Liquid grown plants were harvested, quick frozen in liquid nitrogen, ground to a fine powder with dry ice in a coffee grinder, and either used directly or stored at −70°C. Frozen plant powder was mixed with an equal amount (w/v) of homogenization buffer (100 mM Tris pH 7.5, 10 mM EDTA, 10% glycerol, 150 mM NaCl, and complete protease inhibitor cocktail tablet added fresh as *per* manufacturer's recommendations (Roche)). The homogenate was filtered through four layers of cheesecloth pre-soaked in ice-cold homogenization buffer into a pre-chilled flask on ice. The filtrate was then centrifuged at 6000 × *g* for 15 min at 4°C to pellet intact organelles and cell-wall debris. The supernatant containing membranes and soluble proteins was then centrifuged at 112 000 × *g* for 1 h at 4°C in a swinging bucket rotor to pellet membranes. Membrane pellets were resuspended in resuspension buffer (100 mM Tris pH 7.5, 10% glycerol, 1mM PMSF) homogenized in a dounce homogenizer and stored at −70°C. To 37.5 mL of the soluble supernatant fraction, 500 μL of 50% slurry of IgG sepharose 6 fast flow (GE Healthcare) pre-washed with 3 × 5 mL IgG-W (10 mL Tris, pH 7.5, 150 mM NaCl) was added and the mixture rocked at 4°C for 2 h. Sepharose beads were then pelleted at 200 × *g* for 10–20 s, the supernatant was removed (unbound fraction), and beads were washed with 3 × 5 mL IgG-W.

Fusion proteins were then eluted from the sepharose beads by cleavage with 2 μM (50 μg/500 μL) GST purified GST-TSPN-S2 in cleavage buffer (IgG-W +0.1 mM β-Mercaptoethanol) for 2 h at 16°C. Sepharose beads were

 

pelleted, and supernatant removed and stored at −70°C (first elution). To the sepharose beads, another 2 μM TSPN was added in cleavage buffer and the reaction was allowed to proceed overnight at 16°C before collecting a second elution. The 2 h and 16 h cleavage reactions were then pooled, mixed with 25 μL packed glutathione agarose beads (pre-washed with IgG-W (Sigma)) and incubated for 10 min at 4°C. The slurry was transferred to a spin column (Bio-Rad) and the flow through collected *via* centrifugation at 200 × *g* at 4°C for 10 s. This GST binding step was performed in order to help remove contaminating proteins carried over from the GST-TSPN-ST protease elution step. After a GST clean-up, NaCl was added to the flow through to bring the concentration to 300 mM NaCl and mixed with 100 μL of a 50% slurry of Ni-NTA superflow (Qiagen) pre-washed with 3 × 2 mL 6H-W1 (20 mM Tris-HCl, pH 7.5, 300 mM NaCl). Binding was allowed to proceed at 4°C for 1 h. The mixture was then transferred to a bio-spin column (Bio-Rad), washed with 3 × 1 mL 6H-W1, followed by 2 × 75 μL washes with 6H-W1 +0.1% NP-40 to aid in the removal of non-specific interactions. The column was then washed 2 × 75 μL with 6H-W1 to remove traces of NP-40, and purified protein complexes were eluted from the column with 2 × 100 μL 6H-elution buffer: 20mM Tris-HCl, pH 7.5, 50 mM NaCl and 300 mM imidazole.

### 2.5 Western blot detection of 14-3-3 omega-YFP-TAP2 bait and GFP-TAP2 proteins

Western blotting was performed essentially as described [19]. Briefly, protein samples were mixed with 3 × loading dye and incubated for 10 min at 37°C. Samples were electrophoresed through an 10% polyacrylamide gel (29:1, acrylamide:bisacrylamide, Sigma) and transferred to nitrocellulose using a Bio-Rad transfer apparatus. Blots were incubated in blocking buffer (10 mM Tris, pH 7.6, 137 mM NaCl, 0.5% v/v Tween 20 (TBS-T), with 5% w/v non-fat dry milk) for at least 1 h at RT with shaking followed by a 1 h incubation at RT with primary anti-GFP antibody (Clonetech). After washing, the blots were washed 4 × 10 min in TBS-T and incubated for 1 h at RT with secondary antibody diluted 1:10 000 in blocking buffer. The secondary antibody used for detection was a donkey anti-rabbit IgG conjugated with HRP (GE Healthcare). Following secondary antibody incubation, the blots were washed four times for 10 min in TBS-T, and detection was made using ECL (GE Healthcare).

### 2.6 2-DE and imaging

2-DE was performed as previously described [20]. Purified protein samples were precipitated with 4 volumes of cold (−20°C) acetone. After incubation at −20° overnight, the precipitates were washed twice with −20°C acetone/water (4:1) and resulting pellets were dried for 15 min using a Speed Vac. The pellets were dissolved in 200 μL DeStreak Rehydration Solution (GE Healthcare) and spun at 16 000 rpm at 22°C for 10 min. Bio-Lyte 3–10 Ampholyte (Bio-Rad) was added to each supernatant to a final concentration of 0.2% v/v. 185 μL of each extract (81 μg for 14-3-3 and 97.1 μg for GFP) was loaded onto a 3–10 L (linear) 11 cm IPG strip (Bio-Rad, Hercules, CA) by overnight passive rehydration. Isoelectric focusing was carried out on a Bio-Rad Protean IEF cell using a program as follows: 250 V, linear ramp for 20 min; 8000 V, linear ramp for 2 h 30 min; and 8000 V for a total of 20 000 Vh. Strips were stored at −80°C overnight, then thawed the next day and incubated twice for 10 min each in 8 M urea, 2% SDS, 0.05 M Tris-HCl, pH 8.8, 20% glycerol. The first incubation contained 2% DTT and the second contained 2.5% iodoacetamide. The strips were then layered on 8–16% acrylamide Criterion Tris-HCl gels and embedded in place with 0.5% agarose, along with electrophoresis until the dye front reached the bottom of the gel. Gels were washed with two changes of water (10 min each) and stained overnight with Sypro Ruby stain (Molecular Probes). Stained gels were imaged on a Bio-Rad VersaDoc imager. Images of gels were compared using Bio-Rad PDQuest version 7.3 software and spot sets were created.

### 2.7 In-gel and in-solution protease digestion of proteins

In-gel digestion was performed and modified as previously described [21]. The 2-D-gel spots were excised individually by a ProteomeWorks Spot Cutter (Bio-Rad). Gel samples were washed twice with 25 mM ammonium bicarbonate and 100% ACN, and reduced by 10 mM DTT and alkylated by 100 mM iodoacetamide. Samples were subjected to *in-gel* digestion by incubation with 75 ng trypsin (Promega) dissolved in 25 mM ammonium bicarbonate at 37°C for 6 h on the Investigator ProPrep Digestion and Mass Spec Preparation Station (Genomics Solutions, Ann Arbor, MI). Peptide samples were spotted onto MALDI plates using Zip-Tip μC18 tips (Millipore). 0.5 μL and 0.5 μL matrix mix (5 mg/mL CHCA with 10 mM ammonium phosphate) were then spotted onto the plate.

For in-solution digestion, TAP-affinity purified 14-3-3 and GFP protein complexes were digested by trypsin (Promega) in small aliquots. For each protein sample aliquot (5 μg in 20 μL), 30 μL of 100% ACN was added and incubated for 20 min at RT, followed by the addition of 40 μL 10 mM DTT in 25 mM ammonium bicarbonate and incubation for 10 min at 60°C. After cooling to RT (15 min), 20 μL of 55 mM iodoacetamide in 25 mM ammonium bicarbonate was added and incubation continued for 35 min at RT. Proteolysis was initiated by the addition of 35 μL (0.2 μg) trypsin ((Promega), dissolved in 25 mM ammonium bicarbonate) *per* aliquot reaction and incubated overnight at 37°C.

 

### 2.8 Peptide desalting by reverse phase μC18 Zip-Tip columns

Peptide desalting was performed as previously described [22]. The digested peptides were dried in a vacuum. Desalting of the pellets was performed by use of reverse phase Zip-Tip μC18 columns (Millipore). The C18 column was equilibrated by 100% ACN and washed by 0.1% v/v TFA (in water) three times. Peptide pellet was resuspended in 0.1% v/v TFA and bound onto the column. The C18 column was washed by 0.1% v/v TFA three times and peptides were eluted by a solution containing 50% v/v ACN, 0.1% v/v TFA. The eluate was dried in a speed-vac.

### 2.9 MS analysis and protein identification

2-D gel MS data were collected using an ABI 4700 Proteomics Analyzer MALDI TOF/TOF mass spectrometer (Applied Biosystems, CA), using their 4000 Series Explorer software v. 3.0–3.6. MS acquisition/processing settings were: Reflector Positive Mode (1-keV accelerating voltage), 700–4000 Da acquisition mass range, baseline subtraction enabled at peak width 50, $S/N$ threshold 3, Cluster Area $S/N$ Optimization enabled at $S/N$ 3, internal calibration to within 20 ppm using trypsin autolysis peaks 842.51 and 2211.105. The eight most intense ions were selected for MSMS analysis. MSMS acquisition/processing settings were: 70 Da to precursor ion mass range acquisition, precursor window resolution of −1 to +4 Da, CID on, baseline subtraction enabled at peak width 50, $S/N$ threshold 5. Raw data were extracted for protein identification by GPS Explorer Software v. 3.0–3.6 (Applied Biosystems) and analyzed by Mascot v 1.9.05 (Matrix Science) [23] using NCBI nr database (NCBI 2005.03.22) containing 2 367 365 sequences. Analyses were performed as combination MS+MS/MS. Search settings included MS and MS/MS minimum $S/N$ filter 10, peak density filter 50 peaks *per* 200 Da, maximum number of peaks 65. Additional settings were: cleavage enzyme trypsin, variable modifications of oxidation of Methionine and Carbamidomethylation of Cysteines, max 2 missed cleavages, precursor mass tolerance 20ppm, fragment ion mass tolerance 0.2 Da.

For MALDI-based MudPIT analysis, tryptic digested peptides were fractionated by 2-D-LC). The first dimension was separated by a strong cation-exchange (SCX) column (5 μL, 300 Å, 25 mm length, tapered bore 4.0 mm inlet, 1.0 mm outlet) (Michrom Bioresources) using HPLC. The SCX-bound peptides were eluted with four different salt concentrations of ammonium acetate (Table 1) and separated by the second dimension, a reverse phase C18 column (5 μL, 100 Å, 0.1 × 150 nm) (Michrom). For reverse phase LC gradient formation, solvent A, 0.3% v/v formic acid; solution was mixed with solvent C, 90% v/v ACN, 0.3% v/v formic acid to make 80% v/v ACN as final in 1 h at a nanoflow rate of 0.7 μL/min. The eluted peptides were subjected to spotting onto ABI MALDI plates (400/plate) by a ProBot spotting robot (Dionex LC Packings) in CHCA (Sigma) at a rate of one spot every 6 s followed by a MALDI-TOF-TOF MS/MS analysis using the ABI 4700 spectrometer. Matrix was spiked with Insulin B chain and Angiotensin 1-7 clip standards for MALDI calibration. Peptides were spotted onto MALDI plates, with a density of 400 spots *per* plate. Mass range of MS acquisition was set between 700 and 4000 Da. Laser intensity was set at 4500. For MS processing, baseline was subtracted at 50 with $S/N$ of 3. Smoothing was disabled. $S/N$ threshold for cluster area optimization was set at 10. Internal calibration using masses 3494.651 and 899.466 was performed. For MS/MS acquisition, CID was used with

**Table 1.** 14-3-3 and control GFP samples analyzed by MS

| | Sample – prep #[a)] | Quantative analysis[b)] | Separation method | LC elution | MS method |
|---|---|---|---|---|---|
| 1 | GFP – prep1 | n | 2-D PAGE | | MALDI TOF-TOF |
| 2 | 14-3-3 – prep1 | n | 2-D PAGE | | MALDI TOF-TOF |
| 3 | GFP – prep2 | n | 1-D-LC | ACN | ESI ion-trap |
| 4 | 14-3-3 – prep2 | n | 1-D-LC | ACN | ESI ion-trap |
| 5 | 14-3-3 – prep3 | n | n | | n |
| 6 | GFP – prep3 (O18) | n | n | | n |
| 7 | 5+6 | O16/O18 | 1-D-LC | ACN | ESI ion-trap |
| 8 | GFP – prep4 | n | 2-D-LC | A | MALDI TOF-TOF |
| 9 | GFP – prep5 | n | 2-D-LC | B | MALDI TOF-TOF |
| 10 | 14-3-3 – prep4 | n | 2-D-LC | A | MALDI TOF-TOF |
| 11 | 14-3-3 – prep5 | n | 2-D-LC | B | MALDI TOF-TOF |
| 12 | 14-3-3 –prep5(O18) | n | 2-D-LC | B | MALDI TOF-TOF |
| 13 | 9+12 | O16/O18 | 2-D-LC | B | MALDI TOF-TOF |
| 14 | GFP – prep6 | n | n | | n |
| 15 | 14-3-3 – prep6 | n | n | | n |
| 16 | 14+15 | iTRAQ | 2-D-LC | C | MALDI TOF-TOF |
| 17 | 14-3-3 – prep7 | n | TiO2, 1-D-LC | C | ESI ion-trap |

a) Prep #: biological sample replicates.
b) ACN: acetonitrile.

 

laser intensity at 5500. For MS/MS processing, baseline was subtracted at 1000 with *S/N* threshold at 10. Smoothing was disabled. *S/N* threshold for cluster area optimization was set at 15. Top eight abundant peaks *per* spot were selected for MS/MS analysis. MS/MS data obtained were subjected to MASCOT algorithm analysis against SwissProt database (20050303) containing 176 469 sequences and NCBI database (20050322) containing 2 367 365 sequences.

In some cases, a relative comparison of peptide ion frequencies was evaluated in control and 14-3-3 samples using a non-isobaric tag (iTRAQ) strategy. For iTRAQ samples, the mass tolerance for fragmented ion was set at 0.2 Da. Missed cleavage site was set at 1. Met oxidation and Carbamidomethyl Cys were selected for potential protein modification. Protein identification results were inspected by use of GPS TM software version 3.5 (Applied Biosystems). MS/MS spectra were manually inspected to ensure the quality of the identification. At least two peptides *per* protein were documented for protein identification. For iTRAQ analyses, the mass tolerance for precursor ion was set at 150 ppm and for fragmented ion was set at 0.2 Da. Missed cleavage site was set at 1. Parameters set for potential protein modifications included those to account for iTRAQ labeling and Met oxidation.

To further evaluate the confidence of protein identifications, a decoy database [24] with a randomized version of NCBI nr (20050322) containing 2 367 365 sequences and SwissProt (20050303) containing 176 469 sequences was generated. A combined and concentrated database containing both regular and random sequences was generated. The decoy was searched with the same parameters used for a regular database search. A false-positive identification rate (FDR) was calculated as ((FP/(FP+TP))*2) where FP represents false positive and TP represents true positive. The FDR for all searches was calculated using a peptide homology match cut-off threshold of better than E-value 0.1 [25], and is listed in Supporting Information Table 7. The FDR rates were normally less than 0.01, with the worst case exception at 0.06. In all cases, true positives were confirmed to be the best hits in both SwissProt and NCBI databases.

### 2.10 Prediction of protein mass and peptides containing consensus 14-3-3-binding motifs

Gene ontology annotations were characterized by searching ATG number against The Arabidopsis Information Resource (TAIR) gene ontology database (http://www.arabidopsis.org/tools/bulk/go/index.jsp). The molecular mass of each protein was predicted using Compute pI/Mw algorithm (http://ca.expasy.org/tools/pi_tool.html). A bioinformatic analysis was performed to predict 14-3-3 binding peptides of these interacting proteins by use of MotifScan (http://scansite.mit.edu/motifscan.seq.ptml) [26] algorithm followed by a manual evaluation.

### 2.11 Quantitative proteomics analysis using $^{16}O/^{18}O$ and iTRAQ labeling

MS-based quantitative proteomic analysis using $^{16}O/^{18}O$ stable isotope labeling catalyzed by trypsin digestion was performed as described previously [27]. For $^{16}O/^{18}O$ labeling, trypsin dissolved in $H_2^{16}O$ and $H_2^{18}O$ (Sigma) was used. TAP affinity purified 14-3-3 fraction was subjected to in-solution trypsin digestion in $H_2^{16}O$ at 37°C overnight, whereas GFP fraction was subjected to in-solution digestion in $H_2^{18}O$. After the digestion, two samples were combined into a single tube. Peptides were desalted by reverse phase C18 Zip-Tip columns (Millipore) for MS analysis. The $^{16}O$ and $^{18}O$-labeled peptide has theoretical mass difference of 2 and 4 Da. The signal level of $^{16}O$ peak was compared with the background level. Because in TOF-TOF analysis *S/N* threshold for cluster area optimization was set at 10, the background level was calculated by dividing the signal level by 10. The $^{18}O/^{16}O$ ratio was calculated as such: ($^{18}O$ peak signal-background)/($^{16}O$ peak signal-background). The $^{18}O/^{16}O$ ratio was calculated as such: ($^{18}O$ peak signal-background)/background.

iTRAQ labeling was performed as *per* manufacturer's recommended protocol (Applied Biosystems) starting with the acetone precipitation of the TAP affinity purified proteins. The only deviation included two 5 μg additions (instead of one 10 μg addition) of trypsin (supplied in kit, Applied Biosystems). After the first addition of 5 μg trypsin, the samples were incubated at 40°C for 3 h, followed by a second aliquot of 5 μg trypsin and incubation overnight at 37°C to ensure complete trypsin digestion.

To estimate protein concentration after the acetone precipitation *via* the Bradford method [18], an aliquot of each sample (after solublization in dissolution and denaturization buffer (provided in kit)) was dialyzed using mini-dialysis tubes (Pierce) against 1 L 10 mM Tris pH 6.8 at RT for 1 h to eliminate detergents and salts.

iTRAQ-labeled GFP and 14-3-3 samples were combined into a single sample and subjected to MALDI-based 2-D-LC MS/MS analysis. In this case, the SCX-bound peptides were eluted by ten different concentration of ammonium acetate salt (0, 10, 25, 50, 75, 100, 150, 200, 250, 500 mM). The salt eluted peptides were spotted onto individual spot on ten separate MALDI plates with time interval of 6 s at a nanoflow rate of 0.7 μL/min. Four hundred spots were spotted onto each MALDI plate. An MS/MS analysis of top-three abundant peptides in each spot *per* plate was performed to build up exclusion list. The list includes masses of abundant peptides, *i.e.* 14-3-3, GFP, GST, IgG and trypsin (Supporting Information Table 1). A complete MS/MS analyses on top eight abundant peaks *per* spot was performed to retrieve sequence information of less abundant peptides by including the exclusion list. The iTRAQ (117/114) ratio was calculated by correction factor input for the GPS TM software version 3.5 (Applied Biosystems) using 114 as a reference. Although TOF-TOF was set for a theoretical mass selection window of −0.001 to +2 Da for fragmentation analyses, the

 

instrumentation used here was observed to allow significant amounts of contaminants between −1 and +3 Da. Thus, spectra used for iTRAQ quantitation were manually inspected to ensure that the signals corresponding to the peptide being identified and quantified in a fragmentation analysis represented more than 50% of the total signal.

## 3 Results

### 3.1 TAP-tag affinity purification of 14-3-3 protein complexes *in vivo*

A TAP strategy (TAP-tag purification) was used to purify 14-3-3 omega-YFP-TAP2 (called 14-3-3 samples or 14-3-3-TAP2Y) and GFP-TAP2 (called GFP samples) (Fig. 1A) from the soluble extracts of liquid grown transgenic plants. The first affinity purification step was binding to an IgG sepharose column, followed by a TEV protease cleavage elution (Fig. 1B). The second affinity purification was over a Ni-NTA column. A western blot analysis consistently showed at least a 200-fold enrichment of purified 14-3-3-TAP2Y (Fig. 2A) and a 800-fold enrichment of purified GFP, as shown using an anti-GFP antibody (Fig. 2B) to detect the fusion proteins. In experiments used for MudPIT analyses, this enrichment was improved several fold for both samples by including an extra GST removal step to better remove contaminants that had been added during our TEV protease elution from the IgG column. Regardless, in all purifications, the enrichment for the 14-3-3 samples was around fourfold less compared with the GFP control, consistent with the expectation that the 14-3-3 samples contained a large number of 14-3-3 interacting proteins. The TAP purified samples from multiple 14-3-3-TAP2Y and GFP-TAP2 preparations were analyzed by both 2-D-gel separations and MudPIT, providing evidence for more than 131 14-3-3-specific interacting proteins (Tables 2 and 3).

### 3.2 At least ten of the 14-3-3 isoforms interact with 14-3-3-omega-TAP2Y

To identify the major interacting partners for 14-3-3-omega-TAP2Y, the control GFP and 14-3-3 purified samples were separated in a parallel 2-DE analysis and quantified by Sypro Ruby stain (Fig. 3A and B). Protein spots from both gels were excised, digested, and analyzed by MALDI TOF-TOF MS/MS. The major spots common to GFP and 14-3-3 samples were dominated by expected contaminants, such as TEV protease, which was added as a GST-fusion protein during the elution of proteins bound to the IgG sepharose column. However, approximately fifty 14-3-3 sample-specific spots were detected with varying intensity. All of the strongest staining spots were from eight different 14-3-3 isoforms (including a spot predicted to be

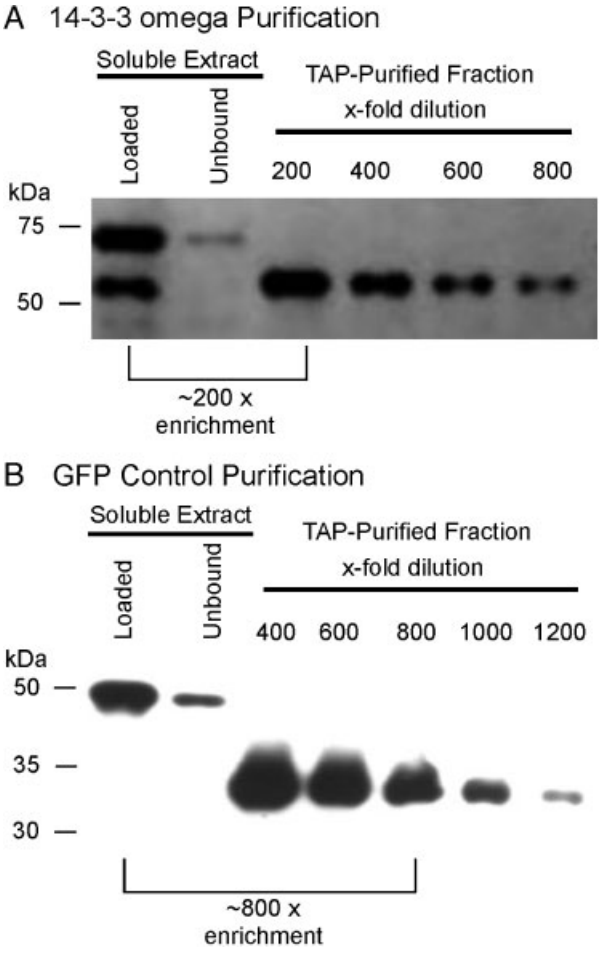


**Figure 2.** Western blots showing an example of enrichment for GFP and 14-3-3 baits in a TAP strategy. Proteins were separated by SDS-PAGE and Western Blots probed with an anti-GFP antibody. For each bait, 50 μg of protein were analyzed to show the signal strength of the GFP in the soluble extract ''loaded'' onto the first IgG purification column, and in the ''unbound'' flow through from that column. Aliquots of the purified fractions were then diluted and analyzed for relative enrichment compared with the starting soluble extract. (A) 14-3-3 purification. (B) GFP control purification. Data represents one replicate of several Western blots used to assess the fold enrichment of independent purifications. 14-3-3 complexes were typically enriched around 200-fold (GFP control, 800-fold) after Protein A and $Ni^{2+}$ purification.

the endogenous omega isoform) (Fig. 3C), as identified by the detection of isoform-specific peptides. In our MudPIT analysis described in MudPIT analyses (Table 1), we also identified two more 14-3-3 isoforms (psi and omicron) (Table 2, Supporting Information Table 2) indicating that our TAP-tagged 14-3-3 omega dimerized with at least 10 of the 12 expressed endogenous 14-3-3 isoforms. Unfortunately, none of the weakly stained spots contained enough protein to generate reliable MS/MS identification results. Nevertheless, this 2-D-gel analysis provided evidence that the complex mixture of copurifying

 

**Table 2.** 14-3-3 isoforms in the 14-3-3 complex

| Protein name | AGI number[a)] | MW (kD)[b)] | Protein score[c)] | Number of replicates[d)] |
|---|---|---|---|---|
| 14-3-3ω (GR14omega) | At1g78300 | 29.1 | 473 | 5 |
| 14-3-3χ (GR14chi) | At4g09000 | 29.9 | 198 | 3 |
| 14-3-3ε (GR14epsilon) | At1g22300 | 28.9 | 240 | 3 |
| 14-3-3κ (GF14kappa) | At5g65430 | 28 | 220 | 3 |
| 14-3-3λ (GF14lambda) | At5g10450 | 27.7 | 129 | 3 |
| 14-3-3 (GF14omicron) | At1g34760 | 27.5 | 133 | 3 |
| 14-3-3φ (GF14phi) | At1g35160 | 30.2 | 585 | 3 |
| 14-3-3μ (GF14mu) | At2g42590 | 28.9 | 210 | 2 |
| 14-3-3ψ (GF14psi) | At5g38480 | 28.6 | 204 | 2 |
| 14-3-3υ (GF14upsilon) | At5g16050 | 30.2 | 598 | 1 |

a) AGI number: the accession number of Arabidopsis genes.
b) MW: predicted molecular mass of the 14-3-3 protein.
c) Protein score: the score the MASCOT software assigned to each identified protein after database searching.
d) Number of replicate: how often a protein identified among different replicates.

14-3-3 clients was not dominated by a few highly abundant proteins, but rather represented a highly diverse mixture of many different proteins, each at a relatively low level of abundance compared with the 14-3-3 proteins.

### 3.3 121 putative 14-3-3 clients were identified by MudPIT analyses

Because the 2-D-gel-based strategy was not sensitive enough to identify any clients in our complex mixture of 14-3-3 interactions, we switched our approach to an in-solution trypsin digestion followed by a 2-D-LC MALDI-based TOF-TOF analysis. Tryptic digested peptides were bound to a SCX column and eluted by different salt concentrations (Table 1). The salt-eluted peptides were separated by a C18 reverse phase column, and peptide fractions were spotted onto MALDI plates for TOF-TOF MS analysis.

As a control for non-specific interactions, we identified proteins that co-purified with our control TAP-tagged GFP in two independent purifications (Table 1). Thirty proteins were identified (Supporting Information Table 3) using a Mascot score of 24 as a reasonable cut-off for a confident database match [28]. Seventy-five percent of these proteins overlapped in both replicates. All of these proteins were considered non-specific contaminating interactions and were therefore excluded from our list below of potential 14-3-3-specific interactions.

To identify putative 14-3-3-specific interactions, we conducted three independent purifications, two of which were done in parallel with GFP controls described above (Table 1). For MS identifications of potential 14-3-3 interactors, we employed the following more rigorous set of criteria. First, we eliminated any protein that overlapped with a putative non-specific interactor in the GFP controls, even if that GFP hit had only been identified as a single peptide with a Mascot score no better than 4, or a confidence as low as 90%. Second, all positive 14-3-3 hits required the identification of at least two peptides, with the final protein identification having a total Mascot score of at least 24, or an overall confidence level of 99%. Third, in 22 cases where the best individual peptide (among the multiple peptides supporting a specific protein identification) had a confidence below 90%, a manual inspection was done to validate the identification. In these cases, at least three immonium ions and three daughter ions (y or b ion) were required to match theoretical mass predictions, and represent the major peaks in the spectra. If more than 50% of the signal in the spectra appeared to be from a contaminating peptide, the spectrum was not used.

Using the above criteria, a total of 131 Arabidopsis proteins were identified as potential interactors with our TAP-tagged 14-3-3 omega (Tables 2 and 3, with details in Supporting Information Tables 2 and 5). Nine of these proteins were identified as specific 14-3-3 isoforms other than omega. Twenty were putative client proteins that were expected based on the plant 14-3-3 interactions reported in the literature (Supporting Information Table 4). These two subsets of interactions confirm that our tagged 14-3-3 formed heterodimers and that these complexes included well-known 14-3-3 clients.

### 3.4 Corroborating 14-3-3 co-purification for 31 clients using quantitative MS

Although 131 proteins were identified in the 14-3-3 purified fraction that were not found in the GFP fraction, 31 selected examples were further shown by quantitative MS strategies to be significantly enriched over background in a 14-3-3 purified sample. This was done by employing two different strategies. This enrichment evidence provides added confidence that a particular 14-3-3 interaction was real, and not just an artifact of not identifying a low-abundance protein in one of the GFP control samples. Although technical limitations prevented a

 

**Table 3.** 14-3-3 Clients identified in the tandem affinity purified14-3-3 samples[a)]

| 14-3-3 Client protein identified (number of replicates)[b)] | ATG number[c)] | Confidence %[d, e)] | Score[f)] |
|---|---|---|---|
| **Carbohydrate metabolism** | | | |
| PEP carboxylase (2) | At1g53310 | 100 | 43 |
| Glucose-6-phosphate dehydrogenase 3 (1) | At1g24280 | 99.9 | 29 |
| Glucose-6-phosphate dehydrogenase 1 (1) | At5g35790 | 99.6 | 27 |
| Acetyl-coenzyme A carboxyl transferase (2) | AtCg00500 | 100 | 43 |
| Fumarase 1 (2) | At2g47510 | 99.9 | 30 |
| Fumarase 2 (1) | At5g50950 | 99.9 | 30 |
| Granule-bound starch synthase I (1) | At1g32900 | 99.8 | 27 |
| Alpha-glucan water dikinase (1) | At1g10760 | 99.9 | 32 |
| Neutral invertase (1) | At1g35580 | 100 | 30 |
| Phosphomannomutase (2) | At2g45790 | 100 | 44 |
| **Nitrogen metabolism** | | | |
| Ferredoxin-dependent Glu synthase 1 (3) | At5g04140 | 100 | 38 |
| Nitrate reductase (2) | At1g77760 | 99.7 | 25 |
| **Transport** | | | |
| Phospholipid-transporting ATPase ALA1 (3) | At5g04930 | 99.1 | 23 |
| Potassium channel GORK (4) | At5g37500 | 99.9 | 32 |
| Cd/Zn translocating ATPase HMA2 (2) | At2g19110 | 100 | 63 |
| Chloride Channel CLC-g (3) | At5g33280 | 96.7 | 23 |
| ADP, ATP carrier protein 2 (1) | At5g13490 | 100 | 52 |
| YCF1.2 Photosystem II component (2) | AtCg01130 | 100 | 54 |
| Plasma membrane H+ ATPase AHA6 (1)[g)] | At2g07560 | 97.1 | 18 |
| **Cytoskeleton** | | | |
| Villin 2 (1) | At2g41740 | 99.8 | 27 |
| Tubulin alpha-6 chain (1) | At4g14960 | 100 | 61 |
| Tubulin beta-8 chain (2) | At5g23860 | 100 | 70 |
| Gamma-tubulin complex component 4 (2) | At3g53760 | 100 | 66 |
| Kinesin-4 (2) | At5g27000 | 100 | 43 |
| Actin 7 (1) | At5g09810 | 100 | 72 |
| ZYP1b, transverse filament-like | At1g22275 | 100 | 46 |
| **Transcription** | | | |
| CURLY LEAF (1) | At2g23380 | 99 | 41 |
| Potential polycomb group protein EZA1 (4) | At4g02020 | 100 | 34 |
| WRKY transcription factor 6 (1) | At1g62300 | 100 | 40 |
| WRKY transcription factor 16 (3) | At5g45050 | 100 | 56 |
| WRKY transcription factor 18 (1) | At4g31800 | 99.9 | 30 |
| WRKY transcription factor 19 (3) | At4g12020 | 100 | 42 |
| WRKY transcription factor 27 (2) | At5g52830 | 99.9 | 28 |
| WRKY transcription factor 32 (4) | At4g30935 | 99.8 | 30 |
| WRKY transcription factor 40 (1) | At1g80840 | 100 | 39 |
| LUMINIDEPZENDENS (3) | At4g02560 | 100 | 37 |
| MADS box protein AGL5 (2) | At2g42830 | 100 | 33 |
| Phytochrome-interacting factor 4 (1) | At2g43010 | 99.9 | 31 |
| DNA-directed RNA pol 3 (3) | At2g24120 | 99.9 | 29 |
| DNA-directed RNA pol beta chain (2) | AtCg00190 | 99.8 | 27 |
| Vernalization-insensitive protein 3 (1) | At5g57380 | 100 | 36 |
| Pirin 1 (1) | At3g59220 | 100 | 35 |
| BAP28 like 18s rRNA maturation factor (4) | At3g06530 | 100 | 61 |
| **Translation** | | | |
| Mitochondria ribosomal protein S4 (2) | AtMg00290 | 100 | 33 |
| Mitochondria ribosomal protein S3 (2) | AtMg00090 | 100 | 40 |
| 40S ribospmal protein S4 (2) | At5g07090 | 100 | 36 |
| 40S ribosomal protein S18 (2) | At1g34030 | 100 | 38 |
| 60S ribosomal protein L2 (1) | At2g18020 | 99.9 | 30 |
| 60S ribosomal protein L26B (1) | At5g67510 | 99.9 | 30 |
| EIF-4A-1 (1) | At3g13920 | 99.9 | 31 |
| EIF-2 beta (2) | At5g20920 | 99.4 | 21 |

 

**Table 3.** Continued

| 14-3-3 Client protein identified (number of replicates)[b)] | ATG number[c)] | Confidence %[d, e)] | Score[f)] |
|---|---|---|---|
| **Signaling** | | | |
| ETO1-like protein 1 (3) | At4g02680 | 100 | 48 |
| ETO1-like protein 2 (3) | At5g58550 | 100 | 37 |
| ACC synthase 6 (1) | At4g11280 | 99.9 | 29 |
| ACC synthase 7 (2) | At4g26200 | 100 | 47 |
| ACC synthase 8 (2) | At4g37770 | 100 | 37 |
| Phospholipase D beta 1 (2) | At2g42010 | 100 | 37 |
| Phospholipase D gamma 1 (2) | At4g11850 | 99.9 | 31 |
| Guanine nucleotide-bind protein (AGB1) (1) | At4g34460 | 99.7 | 26 |
| Inositol-3-phosphate synthase isozyme 1 (1) | At4g39800 | 100 | 40 |
| Inositol-3-phosphate synthase isozyme 2 (2) | At2g22240 | 99.9 | 32 |
| **Kinase** | | | |
| MAP kinase 7 (1) | At2g18170 | 99.6 | 24 |
| Calcium-dependent protein kinase 1 (2) | At5g04870 | 97.7 | 19 |
| Serine/threonine-protein kinase PBS1 (2) | At5g13160 | 100 | 41 |
| Casein kinase II, alpha chain 2 (2) | At3g50000 | 99.8 | 26 |
| Protein kinase AFC1 (1) | At3g53570 | 99.9 | 31 |
| Pantothenate kinase 2 (1) | At4g32180 | 100 | 42 |
| **Phosphatase** | | | |
| S/T-protein phosphatase BSU1 (2) | At1g03445 | 100 | 36 |
| S/T-protein phosphatase BSL1 (2) | At4g03080 | 99.9 | 31 |
| Kinase associated protein phosphatase (3) | At5g19280 | 100 | 34 |
| **Receptors** | | | |
| Glutamate receptor 1.2 (3) | At5g48400 | 99.6 | 32 |
| Glutamate receptor 2.9 (2) | At2g29100 | 100 | 43 |
| Glutamate receptor 3.4 (1) | At1g05200 | 100 | 42 |
| Glutamate receptor 3.7 (2) | At2g32400 | 99.9 | 35 |
| Glutamate receptor 2.1 (2) | At5g27100 | 100 | 33 |
| Receptor protein kinase CLAVATA1 (2) | At1g75820 | 100 | 34 |
| BRI1 receptor kinase (BAK1) (2) | At4g33430 | 99.9 | 28 |
| BRI1-like 2 (1) | At2g01950 | 99.9 | 34 |
| BRI1 (1) | At4g39400 | 99.7 | 28 |
| TOO MANY MOUTH (1) | At1g80080 | 99.8 | 29 |
| **Chaperone** | | | |
| Hsp-60 (3) | At1g55490 | 99.7 | 25 |
| Hsp-101 (3) | At1g74310 | 99.9 | 30 |
| HSP70-2 (1) | At5g02490 | 99.9 | 28 |
| Hsp 81-2 (1) | At5g56030 | 100 | 42 |
| T-complex protein 1, epsioln subunit (3) | At1g24510 | 99.2 | 23 |
| J domain protein (1) | At5g49060 | 100 | 39 |
| **Other** | | | |
| Putative nucleoporin interacting protein (2) | At2g41620 | 100 | 40 |
| LOB domain protein 15 (1) | At2g40470 | 99.9 | 32 |
| Lon protease homolog 2 (4) | At5g26860 | 99.9 | 46 |
| Aspartate carbamoyltransferase (3) | At3g20330 | 100 | 66 |
| PROLIFERA (3) | At4g02060 | 100 | 41 |
| RPP13-like disease resistant protein 1 (3) | At3g14470 | 100 | 40 |
| RPP13-like disease resistant protein 2 (2) | At3g46710 | 100 | 54 |
| Peroxidase 31 (2) | At3g28200 | 100 | 33 |
| Peroxidase 50 (2) | At4g37520 | 99.9 | 36 |
| Peroxidase 51 (1) | At4g37530 | 100 | 34 |
| Peroxidase 52 (3) | At5g05340 | 100 | 38 |
| Disease resistance protein (pCol) (2) | At4g14610 | 100 | 57 |
| Catalase 2 (2) | At4g35090 | 100 | 49 |
| Glycine dehydrogenase (2) | At4g33010 | 100 | 44 |
| Vesicle-fusing ATPase (2) | At4g04910 | 100 | 41 |
| Dynamin 2B (2) | At1g59610 | 100 | 37 |

 

**Table 3.** Continued

| 14-3-3 Client protein identified (number of replicates)[b)] | ATG number[c)] | Confidence %[d, e)] | Score[f)] |
|---|---|---|---|
| DNA topoisomerase I (2) | At5g55300 | 100 | 36 |
| Cytochrome P450 71A23 (2) | At3g48340 | 100 | 33 |
| Glucan endo-1, 3-beta-glucosidase (2) | At3g57260 | 99.8 | 27 |
| D-3-phosphoglycerate dehydrogenase (1) | At1g17745 | 100 | 51 |
| Branched-chain amino acid aminotransferase 1 (1) | At1g10060 | 100 | 47 |
| Cytochrome P450 71A13 (1) | At2g30770 | 100 | 44 |
| Cytochrome P450 86A2 (1) | At4g00360 | 99.9 | 28 |
| Signal recognition particle 54 kD (1) | At5g03940 | 100 | 40 |
| Signal recognition particle 54 kD (1) | At5g49500 | 97.9 | 19 |
| Putative thioredoxin-like 7 (1) | At2g33270 | 100 | 39 |
| GDP-mannose 4, 6 dehydrogenase 1 (1) | At5g66280 | 100 | 38 |
| P-2-dehydro-3-deoxyheptonate aldolase 1 (1) | At4g39980 | 100 | 37 |
| P-2-dehydro-3-deoxyheptonate aldolase 2 (1) | At4g33510 | 99.9 | 33 |
| Cell cycle protein FtsH homolog 1 (1) | At1g50250 | 100 | 37 |
| PP1/PP2A phosphatase pleiotropic regulator (1) | At3g16650 | 100 | 35 |
| Ubiquitin ligase SINAT2 (1) | At3g58040 | 99.9 | 32 |
| FRIGIDA (1) | At4g00650 | 99.8 | 30 |
| Cysteine synthase (1) | At4g14880 | 99.9 | 30 |
| Cysteine synthase (1) | At3g59760 | 100 | 49 |
| Katanin like protein (1) | At5g23430 | 99.6 | 26 |
| Cell division protein 48 homolog E (1) | At5g03340 | 99.8 | 26 |
| GIGANTEA protein (1) | At1g22770 | 99.7 | 26 |
| Serpin (1) | At1g62170 | 99.9 | 21 |
| Lyase (1) | At3g25810 | 99.9 | 68 |
| Putative unconventional myosin (1) | At2g31900 | 99.9 | 98 |
| Glutamyl-tRNA synthase (2) | At5g64050 | 97.5 | 19 |
| YCF1.2 Photosystem II component (2) | AtCg01130 | 100 | 54 |
| DNA repair protein UVH3 (2) | At3g28030 | 100 | 44 |

a) Total peptide number identified is listed in Supporting Information Table 5.
b) Number of replicates: how often a protein identified among different replicates.
c) ATG number: the accession number of Arabidopsis genes.
d) Confidence %: the confidence interval of the identified protein after database searching.
e) Confidence % shown are for protein identification based on MASCOT.
f) Score: the score the MASCOT software assigned to each identified protein after database searching.
g) Only AHA6 has mode III motif.

quantitative enrichment of every putative 14-3-3 client, we never observed a case in which a putative client was also identified in the GFP samples. Thus, all the enrichment ratios are actually based on an increase over varying levels of background noise from contaminating peptide(s).

The first approach was to label 14-3-3 sample peptides with $^{18}O$ during a trypsin digestion. These labeled peptides were then mixed into a single sample with an equal amount of $^{16}O$-labeled peptides from a GFP control purification. This mixed sample was then subjected to a 2-D-LC MALDI-TOF-TOF MS analysis to provide a relative comparison of signal strength for different pairs of $^{16}O/^{18}O$-labeled peptides. This strategy identified nine putative 14-3-3 clients with quantitative evidence for clear enrichment in the 14-3-3 sample (Supporting Information Fig. 4). These include, peroxidase 31, WRKY transcription factor 16, guard cell recycling outward $K^+$ channel (GORK) channel, CURLY LEAF, cadmium/zinc-transporting ATPase 2 (HMA2), glutamate receptor 1.2, CLC-G channel, ALA1 and invertase.

The second approach was to use a quantitative iTRAQ strategy. The 14-3-3 and GFP samples were labeled with either iTRAQ 117 or 114 mass reporters, respectively. The labeled samples were combined and subjected to a 2-D-LC MALDI-TOF-TOF MS analysis (Table 1). As expected, peptides derived from known contaminants, such as added trypsin and GST-TEV protease, showed ratios of 1.1 and 1.4, respectively (Supporting Information Table 6), confirming that the two iTRAQ-labeled samples were mixed equally. By comparing enrichment levels for shared and unique peptides associated with the GFP and 14-3-3 tags, we established normalization criteria for estimating minimum enrichment ratios (Supporting Information Text 1). Using this approach, minimum enrichment ratios from 12 to 243 were found for 21 putative client proteins, including UVH3, phosphoenol pyruvate (PEP) carboxylase, phosphoglucomutase, G-6-P dehydrogenase, Glutamyl-tRNA synthase and phospholipase D alpha (Supporting Information Fig. 5).

 

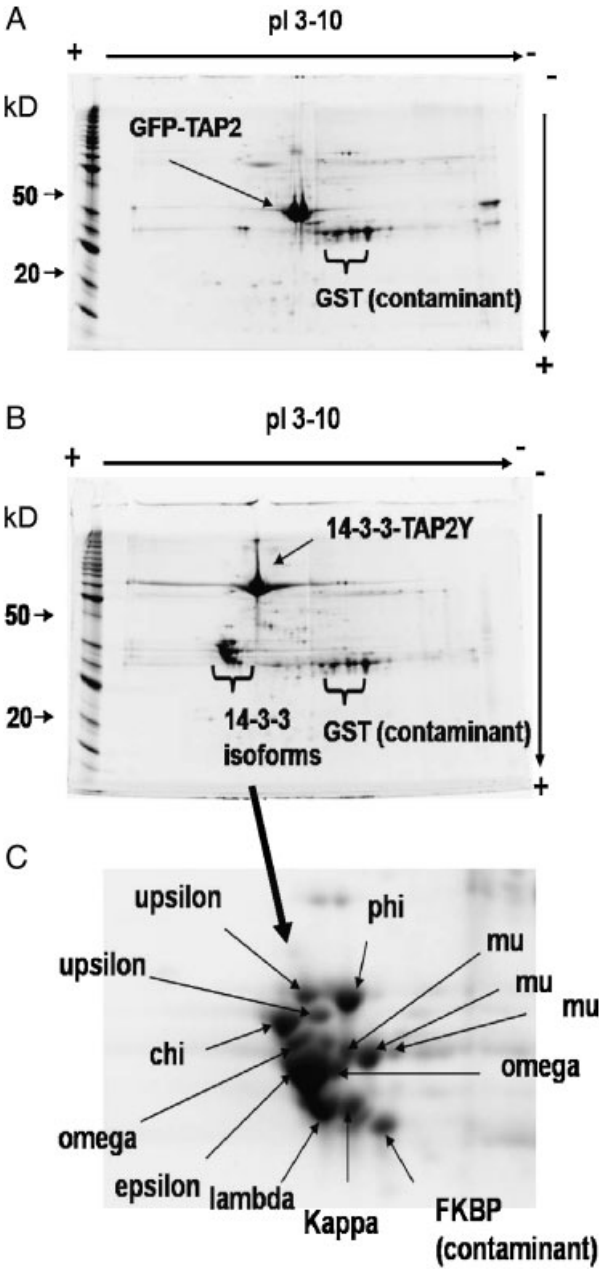


**Figure 3.** 2-D gel electrophoresis fractionation of 14-3-3 protein complexes reveals 14-3-3 isoforms. (A) TAP affinity-purified GFP control. (B) TAP affinity-purified 14-3-3 protein complexes. (C) A region of B showing the 14-3-3 isoforms that co-purified with the bait 14-3-3 omega-YFP-TAP2. Protein gels were stained by Sypro Ruby stain.

## 4 Discussion

The TAP-tag purification strategy used here provides evidence for more than 131 different protein interactions with 14-3-3 omega, ten of which were 14-3-3 isoforms (including itself) and 121 of which are putative 14-3-3 clients. Of these putative clients, 20 were previously reported in the literature. These include such proteins as nitrate reductase, neutral invertase, serpin, calcium-dependent protein kinase-1 (CDPK1/CPK1), and 1-aminocyclopropane-1-carboxylate (ACC) synthase. An additional 101 interactors have not been previously identified, raising the number of putative 14-3-3 clients identified in plants to more than 300 (see Supporting Information Table 4). A current estimate for the number of 14-3-3 interactions in animal systems is also over 300 [8]. Although plants and animals show some 14-3-3 clients in common (such as MAPKs and Glutamate Receptors, discussed below) the vast majority appear unique to either plants or animals. This suggests that 14-3-3 interactions have adapted to provide new regulatory interactions as eukaryotic organisms evolve.

Two lines of evidence suggest that many more interactors are yet to be identified. First, we only detected a 25% overlap with other studies, while still identifying 101 new interactions. Second, preliminary results based on single peptide identifications in this study provide an expectation for more than 100 additional 14-3-3 interactors (data not shown). Identifying all of the 14-3-3 interactions is a formidable challenge, especially because many of the interactions are phospho-dependent, transient and include many low-abundance proteins that are hard to detect.

### 4.1 Identifying 14-3-3 clients with *in vivo* interaction evidence

In plants, most of the putative 14-3-3 interactions have been identified by Y2H strategies or the enrichment of 14-3-3 clients from plant extracts run through a 14-3-3 affinity chromatography column. In relatively few cases have interactions been verified with *in vivo* evidence. One advantage of the TAP-tag strategy used here is that each interactor identified comes with experimental support for an *in vivo* interaction [29].

Although a TAP-tag strategy offers a productive strategy to identify potential clients, an important caveat is that the purification of 14-3-3 complexes may also include non-client proteins that are only indirectly associated with the complex through a secondary binding to a true client. Although we have not conducted *in vitro* binding assays to verify a direct 14-3-3 interaction for any of the new potential clients identified here, most of the proteins do contain a Mode-1 or Mode-2 target-binding site, consistent with typical 14-3-3 clients. Further confirmation may require *in vitro* binding assays in which the client has been phosphorylated by an appropriate protein kinase, and the binding shown to be competitive with a known 14-3-3 peptide substrate, such as a phospho Raf-1 peptide (*e.g.* [30]). Nevertheless, the co-purification of a protein as part of a stable 14-3-3 complex still supports a working hypothesis that its interaction may have *in vivo* regulatory significance.

 

### 4.2 14-3-3 omega can heterodimerize with at least nine other isoforms *in vivo*

Although several studies have reported that 14-3-3 proteins can form heterodimers [2, 11], the extent to which this can occur *in vivo* between omega and the 11 other expressed Arabidopsis isoforms is not fully known. Evidence here indicates that isoform omega can hetero-dimerize *in vivo* with at least nine of the other expressed isoforms. It is not clear if the failure to see an interaction with isoforms iota (GRF12, At1g34760) and nu (GRF7, At3g02520) is a function of unique properties of these isoforms, or a technical limitation of our experimental strategy.

The ability of our tagged 14-3-3 to interact with other isoforms demonstrates that a large C-terminal tag on 14-3-3 omega does not disrupt its hetero-dimerization potential. This is consistent with structure–function studies on 14-3-3s that indicate that the C-terminal end is primarily involved in client interactions (*e.g.* [31]) whereas the N-terminal end mediates dimerization (*e.g.* [32]). A C-terminal location for a TAP-tag was also used in an animal study that successfully identified 117 interactions [10]. Although we cannot rule out that a C-terminal TAP-tag will modify some client-binding interactions, the fact that heterodimers are formed with at least nine other endogenous Arabidopsis 14-3-3 isoforms (which have an un-modified C-terminal domain) provides an expectation that most clients will still interact with the un-tagged half of the heterodimer, and therefore be detected by our experimental strategy.

### 4.3 Identification of 16 membrane proteins as 14-3-3 clients

Among the 121 putative clients identified here, 16 (13%) have evidence for membrane association. This increases by fourfold the number of membrane proteins in plants with evidence for a 14-3-3 interaction. Based on our experimental design, membrane proteins were not expected to be highly represented because our protocol discarded membrane proteins that were pelleted during a high-speed centrifugation. Nevertheless, partial proteolysis of membrane proteins is common in plant protein purifications. In our study, it appears that partial proteolysis produced a significant number of ''shaved'' protein fragments that retained their binding interaction with the TAP-tagged 14-3-3. An alternative explanation is that we simply purified a small number of membrane vesicles and identified abundant proteins associated with such vesicles. This appears unlikely for three reasons. First, our GFP control purifications showed no examples of an abundant integral membrane protein contaminant. Second, in the 14-3-3 samples, we saw no evidence for a general enrichment for some of the most abundant membrane associated or compartmentalized proteins, such as the chloroplast inner envelope proteins, BiP (an ER luminal protein), or RUBP-carboxylase. Finally, for each of the 16 integral membrane proteins identified, all of the peptides detected by mass spectrometry map to the cytosolic exposed face of the protein, according to topology models found at (http://aramemnon.botanik.uni-koeln.de/index.ep) [33]. This bias for cytosolic exposed peptides is most consistent with a protocol that selectively purified 14-3-3-bound protein fragments that were released by partial proteolysis, as opposed to a general non-specific recovery of abundant proteins associated with membrane vesicles.

Evidence that our protocol successfully purified known 14-3-3 membrane protein interactions was provided by the identification of a plasma membrane $H^+$-ATPase (AHA6), one of the most well-studied 14-3-3 target interactions in plants [6, 34]. Three new groups of 14-3-3 membrane complexes (including $K^+$, $Ca^{2+}$, and $Cl^-$ channels) are highlighted in the next section.

### 4.4 Biological implications

The 14-3-3 interactions detected here have implications to many aspects of plant biology, confirming the diversity of interactions identified by previous 14-3-3 target surveys [35–39]. However, for each new putative client, the challenge will be to verify a direct 14-3-3-specific interaction and determine its functional consequence. The literature provides a precedent for 14-3-3 interactions resulting in: (i) enzyme activation and inactivation (*e.g.* $H^+$-ATPase and nitrate reductase, respectively [34], (ii) masking or unmasking of protein targeting information (*e.g.* Bzr1 transcription factor [40, 41], (iii) bridging or blocking the formation of protein complexes [8]. From our list of 131 interactions, we offer a few examples below that highlight potential clients of special interest.

#### 4.4.1 Channels for $K^+$ and $Cl^-$

The $K^+$ ion channel GORK was identified here in three independent 14-3-3 co-purifications and appeared with a greater than 109-fold enrichment over background in our $^{18}O/^{16}O$ 14-3-3/GFP comparison. GORK is a plasma membrane $K^+$ channel, with one of its biological functions linked to the regulation of stomatal aperture and transpiration [42, 43]. 14-3-3 s have previously been proposed as a master regulator of ion homeostasis across the plasma membrane, with evidence for regulation of the plasma membrane proton pump as well as $K_{in}$ and $K_{out}$ channels [44]. More recently, 14-3-3 has been implicated in the regulation of two specific $K^+$ channels, AtTPK1 (KCO1), a vacuolar membrane localized $K^+$ channel [45] and KAT1, a PM inward rectifying $K^+$ channel [46].

A putative chloride channel, CLCg, was also identified here in two independent co-purifications, with a greater than 47-fold enrichment over background in our $^{18}O/^{16}O$ 14-3-3/GFP comparison. Although the sub-cellular localization of CLCg is not yet known [47], the regulation of $Cl^-$

 

and $K^+$ transport are expected to be linked in some situations requiring a net balance of positive and negative charges moving across the membrane. Our results raise the potential that 14-3-3 may be involved in a mechanism to coordinate the regulation of $K^+$ and $Cl^-$ transport across different membranes.

#### 4.4.2 Glutamate receptors

Strong evidence was obtained here for 14-3-3 interactions with five different glutamate receptor isoforms (GLRs 1.2, 2.1, 2.9, 3.4 and 3.7) representing all three major subgroups. Isoform GLR1.2 was found in two independent purifications and displayed a greater than 519-fold enrichment over background in our $^{18}O/^{16}O$ 14-3-3/GFP comparison. In Arabidopsis, glutamate receptors are implicated in calcium signaling and are represented by 20 isoforms [48–51]. All five GLRs identified here display a Mode-1 or Mode-2 14-3-3 binding site. Of the 20 Arabidopsis isoforms, all but three (*i.e.* 17) have potential Mode-1 or -2 binding sites, suggesting that 14-3-3 interactions might be a common feature for most members of this family in plants. In animals, glutamate receptors have also been identified as 14-3-3 clients [11] providing a potential example of a common target of 14-3-3 regulation in both plants and animals.

#### 4.4.3 Ethylene biosynthesis

Evidence for 14-3-3 interactions was found for a subset of proteins all linked to the biosynthesis of ethylene, including three isoforms of ACC synthase (ACS-6, 7, 8), an ETO-like protein, and S-adenosylmethionine synthase. Although not confirmed by a second peptide identification, preliminary evidence indicates a potential 14-3-3 interaction with ethylene insensitive3. Ethylene insensitive3 is a transcription factor that plays an important role in ethylene signaling [52]. The identification here of ACC synthase provides *in vivo* corroboration for an ACC synthase interaction previously identified by an *in vitro* binding reaction with barley 14-3-3 proteins [53] and rice 14-3-3 proteins [54]. ACC synthase is a key enzyme in ethylene biosynthesis, and is known to be regulated through binding of a protein called ETO1 [55]. Regulation of ACC synthase activity by CDPK phosphorylation has also been proposed, providing a potential link between stress-induced calcium signals and the biosynthesis of ethylene [56]. Some CDPKs have also been found to bind to a 14-3-3 [30]. This group of interactions raises a number of questions, such as whether CDPK phosphorylation promotes binding of 14-3-3 to ACS and ETO, and whether ETO and 14-3-3 have an antagonistic relationship with respect to regulating ACS. Regardless, these results suggest that multiple 14-3-3 interactions could have significant impacts on ethylene signaling.

#### 4.4.4 Transcription

Based on previous studies, 14-3-3 proteins have been implicated in the regulation of transcription through interactions with transcription factors [57]. A total of 15 transcription factors were identified here as putative clients. The largest subgroup of transcription factors belonged to the WRKY family (isoforms, 6, 16, 18, 19, 27, 32 and 40), implicated in regulating many different sets of genes, some of which are linked to biotic and abiotic stress pathways [58]. For example, AtWRKY6 expression changes during leaf senescence and pathogen defense [59]. In addition, AtWRKY18 and AtWRKY40 are involved in disease resistance [60]. Of the seven WRKYs identified here, all but one of them have at least one consensus 14-3-3 binding motif. WRKY-16 has seven consensus binding sites.

#### 4.4.5 Chaperones

Another major subgroup of 14-3-3 interactions belongs to different chaperones, such as the HSP family (HSP60, HSP70, HSP81, and HSP101), a J Domain Protein, and T-complex protein-1. Because some chaperones are known to bind to many proteins, it is not clear if these interactions are non-specific or involve a specific 14-3-3 binding site. However, two of the HSPs (HSP60 and HSP70) do have consensus 14-3-3 binding sites. Furthermore, a barley HSP60 ortholog was previously identified as a client protein by affinity chromatography [35]. Because this barley study eluted 14-3-3-interactors by competition with a client peptide, this experimental design supports an interpretation that the barley HSP60 ortholog was identified as a true 14-3-3 client rather than a non-specific interaction. If *in vitro* binding assays eventually confirm some of the chaperones identified here as true 14-3-3 clients, this would dramatically expand the 14-3-3 interactome to include indirect associations with a large fraction of the proteome that have chaperone interactions.

#### 4.4.6 Carbohydrate metabolism

Multiple clients have been found in several linked steps in carbohydrate metabolism [35]. The identification here of PEP carboxylase provides a novel and significant addition to the emerging connections in this metabolic pathway. PEP carboxylase was found in two independent purifications and displayed a greater than 242-fold enrichment over background in our $^{18}O/^{16}O$ 14-3-3/GFP comparison. PEP carboxylase, which catalyzes the assimilation of $CO_2$ into a four-carbon compound oxaloacetate, functions in many aspects of metabolism, including (in a C3 plant such as Arabidopsis) replenishment of tricarboxylic acid cycle intermediates, pH control, carbon and nitrogen partitioning, and malate synthesis [61]. Although phospho-regulation of

 

PEP-carboxylase is well established, an additional role for 14-3-3 now appears to warrant consideration. Because PEP-carboxylase does not have a consensus 14-3-3 binding site, alternative non-consensus sites may be involved, such as RLFSVD or RLATPE, as predicted by (http://elm.eu.org/). Alternatively, binding may involve an already established phospho-regulatory site near the N-terminal end (consensus = (E/D)(R/K)xxSIDAQ(L/M)R) (where x represents any amino acid and the $S_p/T_p$ is phosphorylated), which does show similarity to a Mode-1 consensus 14-3-3 binding site.

#### 4.4.7 Translation

A role for 14-3-3 in protein synthesis was previously proposed based on interactions with translation initiation factors, as shown by co-immunoprecipitation and *in vitro* translation assays in which 14-3-3 was depleted [62]. Here we provide additional evidence with the identification of several ribosomal proteins (r-proteins) (*i.e.* 40S r-protein S4 and S18; 60S r-protein L8 and L26B) as well as regulatory proteins, eIF4A and eIF2. A previous proteomics analysis of a purified polysomal mRNA fraction also produced evidence for an association with 14-3-3 phi [63].

#### 4.4.8 Phospholipase D signaling

Phospholipase D activity has been implicated in regulating multiple pathways, including those that control cell growth and patterning, programmed cell death, vesicle trafficking, cytoskeletal organization and abiotic stress [64–69]. Here we identified two phospholipase D proteins (beta and gamma) as potential 14-3-3 clients, consistent with expectations from phospholipase/14-3-3 interactions documented in animal systems [70]. Interestingly, a 14-3-3 has also been shown to bind phosphatidic acid (PA) [71], which is a signaling molecule [72] generated from phospholipase D. In plants, PA was also shown to interact with PEP carboxylase [71], which was identified here as a potential 14-3-3 client. This unexpected interconnection of 14-3-3, PA, and PEP-carboxylase, raises the question of whether other targets of PA may also be connected to 14-3-3 in some feedback regulatory network. Regardless, phospholipase D has been implicated in stress responses in plants [73] and provides a logical target for considering mechanistic models in which 14-3-3 helps regulate such responses, such as a ''stay green'' drought resistant phenotype seen in cotton [74].

#### 4.4.9 Phospho-signaling

Because most 14-3-3 interactions are thought to be mediated by target site phosphorylation, a comprehensive understanding of the 14-3-3 interactome will require delineating the kinases and phosphatases that regulate 14-3-3 interaction dynamics. Although kinases provide an upstream trigger that can potentiate many 14-3-3 binding interactions, they also appear to be well represented as downstream clients. Of the 121 putative clients identified here, six were members of various protein kinase families (Table 3).

#### 4.4.10 A 14-3-3/serine-threonine plant receptor kinase signaling module

Our investigation provides *in vivo* 14-3-3 interaction evidence for both subunits of the brassinosteroid receptor, BRI1 and BAK1, both of which are members of a large family of LRR-receptor kinases. Previous studies have identified a 14-3-3 interaction with BAK1 by use of Y2H screen, and obtained support for an *in vivo* interaction through immuno-precipitation [75, 76]. However, a direct Y2H test for a similar 14-3-3 interaction with the BRI1 subunit failed to show an interaction [41]. We offer two explanations for the failure of a Y2H strategy to detect a BRI1/14-3-3 interaction in difference to our success using a TAP-tag co-purification strategy. The first is that the interaction does not occur in yeast because the putative target-binding site on BRI1 was not being phosphorylated. Second, our *in planta* interaction may be detecting an indirect interaction that is mediated by the association of a proteolytic fragment of BRI1 with a non-client binding site associated with a BAK1/14-3-3 complex. Regardless, there is strong evidence that the brassinosteroid response pathway is regulated downstream of BRI1/BAK1 through a 14-3-3 interaction with the transcription factor BZR1, which when phosphorylated binds a 14-3-3, causing it to be retained in the cytoplasm [40, 41].

Our study also identified a related BRI1-like receptor kinase, two additional leucine repeat receptor kinases, and clavata, which is involved in shoot and floral meristem development. Another example of a 14-3-3 interaction with a fifth LRR-receptor kinase (SERK1) has been found through a Y2H study, with confirmation of an *in vivo* interaction provided by a FRET strategy using CFP and YFP tags [75].

The growing number of 14-3-3/LRR-receptor kinase interactions suggests that 14-3-3 interactions may have co-evolved with a subset of the plant receptor kinase as a regulatory module. Unlike typical animal receptor kinases, which are predominately tyrosine kinases, the plant receptor kinases are Ser/Thr kinases, and are therefore candidates for phospho-regulation through auto-regulation of Mode-1 and Mode-2 14-3-3 binding sites.

#### 4.4.11 A MAPK signaling module

Our investigation provides *in vivo* evidence for a 14-3-3 interaction with AtMAPK7. *In vitro* binding studies have documented a 14-3-3 interaction with an auto-phosphory-

 

lated MAPK from maize (ZmMPK6) [77]. In yeast, there is evidence for 14-3-3 regulation of two MAPK pathways, one that functions in pseudo-hyphal development (RAS/Kss1-MAPK) [78] and one in osmotolerance (Hog1/MPK1). These interactions have been proposed as part of an explanation for why yeast with reduced 14-3-3 expression cannot grow under several stress conditions. MAPK/14-3-3 interactions are also established in mammalian systems, such as MEK kinase interactions with 14-3-3 zeta and epsilon in animals [79]. For AtMAPK7, a peptide containing only a consensus 14-3-3 binding site (RFIKSLP) has also been found to be an excellent peptide substrate for phosphorylation by a CDPK (Harper, unpublished observations). This raises an interesting hypothesis that calcium signals may influence some MAPK signaling pathways through CDPK-mediated MAPK/14-3-3 interactions.

#### 4.4.12 Chloroplast and mitochondrial functions

Several examples have been reported for 14-3-3 protein interactions within the mitochondria and chloroplast (*e.g.* [80–82]). For example, evidence indicates that a 14-3-3 can regulate the activity of the ATP synthase in both chloroplasts and mitochondria [81]. Here we identified two plastid and two mitochondrial encoded proteins as potential clients of 14-3-3 omega (*e.g.* an acetyl-coenzyme A carboxyl transferase in the chloroplast). Although it is not clear how 14-3-3 omega is translocated into these organelles, our results support previous research indicating important functional roles for 14-3-3 within the mitochondria and chloroplast.

## 5 Concluding remarks

The size of the 14-3-3 interactome has now exceeded 300 putative clients each in yeast, mammals and plants. Each organism's client list reveals similar regulatory themes. For example, all three groups show evidence for an ancient 14-3-3/MAPK signaling module. However many clients appear to be phylogenetically unique. For example, several clients identified here belong to kinase families not found in animals or yeast, such as the LRR-Ser/Thr receptor kinases and CDPKs. This phylogentic diversity of clients supports a perspective that 14-3-3 interactions are continuing to evolve into new functional partnerships.

Because the 12 different 14-3-3s expressed in Arabidopsis can potentially dimerize into 78 different complexes, and each 14-3-3 dimer can bind two different clients, the potential number of different 14-3-3/client complexes that can be formed with more than 300 different clients could theoretically exceed a million. Adding to this potential complexity is the fact that some of the putative clients have multiple binding interactions of their own. For example, a 14-3-3 interaction with one of the chaperones may indirectly link 14-3-3 with a very large percentage of the proteome. Thus, 14-3-3s may represent one of the busiest and most dynamic interaction nodes in the emerging global map of eukaryotic protein–protein interactions.

*This work was supported by grants to J.F.H. from NSF (MCB-0114769, DBI-0420033 and DBI-0436450), the DOE (DE-FG03-94ER20152) and NIH 1RO1 GM070813-01 for the development of the affinity tagging system, and to IFC from National Science Council, Taiwan (NSC96-3111-B-002-001 and NSC97-2311-B-002-005-MY3). We appreciated the help from Technology Commons, College of Life Science, National Taiwan University. Mass Spectrometry and Bioinformatics were made possible by the INBRE Program of the National Center for Research Resources (NIH grant P20 RR-016464).*

*The authors have declared no conflict of interest.*

## 6 References

[1] Rosenquist, M., Alsterfjord, M., Larsson, C., Sommarin, M., Data mining the Arabidopsis genome reveals fifteen 14-3-3 genes. Expression is demonstrated for two out of five novel genes. *Plant Physiol.* 2001, *127*, 142–149.

[2] Fuller, B., Stevens, S. M., Jr., Sehnke, P. C., Ferl, R. J., Proteomic analysis of the 14-3-3 family in Arabidopsis. *Proteomics* 2006, *6*, 3050–3059.

[3] Sehnke, P. C., Rosenquist, M., Alsterfjord, M., DeLille, J. *et al.*, Evolution and isoform specificity of plant 14-3-3 proteins. *Plant Mol. Biol.* 2002, *50*, 1011–1018.

[4] Muslin, A. J., Tanner, J. W., Allen, P. M., Shaw, A. S., Interaction of 14-3-3 with signaling proteins is mediated by the recognition of phosphoserine. *Cell* 1996, *84*, 889–897.

[5] Yaffe, M. B., Rittinger, K., Volinia, S., Caron, P. R. *et al.*, The structural basis for 14-3-3: phosphopeptide binding specificity. *Cell* 1997, *91*, 961–971.

[6] Maudoux, O., Batoko, H., Oecking, C., Gevaert, K. *et al.*, A plant plasma membrane $H^+$-ATPase expressed in yeast is activated by phosphorylation at its penultimate residue and binding of 14-3-3 regulatory proteins in the absence of fusicoccin. *J. Biol. Chem.* 2000, *275*, 17762–17770.

[7] Ottmann, C., Yasmin, L., Weyand, M., Veesenmeyer, J. L. *et al.*, Phosphorylation independent interaction between 14-3-3 and exoenzyme S: from structure to pathogenesis. *EMBO J.* 2007, *26*, 902–913.

[8] van Heusden, G. P., 14-3-3 proteins: regulators of numerous eukaryotic proteins. *IUBMB Life* 2005, *57*, 623–629.

[9] Jin, J., Smith, F. D., Stark, C., Wells, C. D. *et al.*, Proteomic, functional, and domainbased analysis of in vivo 14-3-3 binding proteins involved in cytoskeletonregulation and cellular organization. *Curr. Biol.* 2004, *14*, 1436–1450.

[10] Benzinger, A., Muster, N., Koch, H. B., Yates, J. R., III, Hermeking H., Targeted proteomic analysis of 14-3-3 sigma, a p53 effector commonly silenced in cancer. *Mol. Cell. Proteomics* 2005, *4*, 785–795.

 

[11] Angrand, P. O., Segura, I., Volkel, P., Ghidelli, S. *et al.*, Transgenic mouse proteomics identifies new 14-3-3 associated proteins involved in cytoskeleton rearrangements and cell signaling. *Mol. Cell. Proteomics* 2006, *5*, 2211–2227.

[12] Wang, D., Harper, J. F., Gribskov, M., Systematic transgenomic comparison of protein kinase between Arabidopsis and *Saccharomyces cerevisiae*. *Plant Physiol.* 2003, *132*, 2152–2165.

[13] Morsy, M., Gouthu, S., Orchard, S., Thorneycroft, D. *et al.*, Charting plant interactomes; possibilities and challenges. *Trends Plant Sci.* 2008, *13*, 183–191.

[14] Clough, S. J. and Bent, A. F., Floral dip: a simplified method for Agrobacterium mediated transformation of *Arabidopsis thaliana*. *Plant J.* 1998, *16*, 735–743.

[15] Lucast, L. J., Batey, R. T., Doudna, J. A., Large-scale purification of a stable form of recombinant tobacco etch virus protease. *Biotechniques* 2001, *30*, 544–546, 548, 550 *passim*.

[16] Hellens, R. P., Allan, A. C., Friel, E. N., Bolitho, K. *et al.*, Transient expression vectors for functional genomics, quantification of promoter activity and RNA silencing in plants. *Plant Methods* 2005, *1*, 13.

[17] Bevan, M., Binary Agrobacterium vectors for plant transformation. *Nucleic Acids Res.* 1984, *12*, 8711–8721.

[18] Bradford, M. M., A rapid and sensitive method for the quantation of protein utilizing the principle of protein-dye binding. *Anal. Biochem.* 1976, *72*, 248–254.

[19] Curran, A. C., Hwang, I., Corbin, J., Martinez, S. *et al.*, Autoinhibition of a calmodulin-dependent calcium pump involves a structure in the stalk that connects the transmembrane domain to the ATPase catalytic domain. *J. Biol. Chem.* 2000, *275*, 30301–30308.

[20] Yamamoto-Mizuma, S., Wang, G. X., Liu, L. L., Schegg, K. *et al.*, Altered properties of volume-sensitive osmolyte and anion channels (VSOACs) and membrane protein expression in cardiac and smooth muscle myocytes from *Clcn3*-/- mice. *J. Physiol.* 2004, *557*, 439–456.

[21] Rosenfeld, J., Capdevielle, J., Guillemot, J. C., Ferrara, P., In-gel digestion of proteins for internal sequence analysis after one- or two-dimensional gel electrophoresis. *Anal. Biochem.* 1992, *203*, 173–179.

[22] Williams, A. J., Werner-Fraczek, J., Chang, I. F., Bailey-Serres, J., Regulated phosphorylation of 40S ribosomal protein S6 in root tips of maize. *Plant Physiol.* 2003, *132*, 2086–2097.

[23] Perkins, D. N., Pappin, D. J., Creasy, D. M., Cottrell, J. S., Probability-based protein identification by searching sequence database using mass spectrometry data. *Electrophoresis* 1999, *20*, 3551–3567.

[24] Elias, J. E., Haas, W., Faherty, B. K., Gygi, S. P., Comparative evaluation of mass spectrometry platforms used in large-scale proteomics investigations. *Nat. Methods* 2005, *2*, 667–675.

[25] Thompson, M. R., Thompson, D. K., Hettich, R. L., Systematic assessment of the benefits and caveats in mining microbial post-translational modifications from shotgun proteomic data: the response of *Shewanella oneidensis* to chromate exposure. *J. Proteome Res.* 2008, *7*, 648–658.

[26] Obenauer, J. C., Cantley, L. C., Yaffe, M. B., Proteome-wide prediction of cell signaling interactions using short sequence motifs. *Nucleic Acids Res.* 2003, *31*, 3635–3641.

[27] Nelson, C. J., Hegeman, A. D., Harms, A. C., Sussman, M. R., A quantitative analysis of Arabidopsis plasma membrane using trypsin-catalyzed (18)O labeling. *Mol. Cell. Proteomics* 2006, *5*, 1382–1395.

[28] Olsen, J. V., Ong, S. E., Mann, M., Trypsin cleaves exclusively C-terminal to arginine and lysine residues. *Mol. Cell. Proteomics* 2004, *3*, 608–614.

[29] Chang, I. F., Mass spectrometry-based proteomic analysis of the epitope-tag affinity purified protein complexes in eukaryotes. *Proteomics* 2006, *6*, 6158–6166.

[30] Moorhead, G., Douglas, P., Cotelle, V., Harthill, J. *et al.*, Phosphorylation dependent interactions between enzymes of plant metabolism and 14-3-3 proteins. *Plant J.* 1999, *18*, 1–12.

[31] Athwal, G. S. and Huber, S. C., Divalent cations and polyamines bind to loop 8 of 14-3-3 proteins, modulating their interaction with phosphorylated nitrate reductase. *Plant J.* 2002, *29*, 119–129.

[32] Abarca, D., Madueno, F., Martinez-Zapater, J. M., Salinas, J., Dimerization of Arabidopsis 14-3-3 proteins: structural requirements within the N-terminal domain and effect of calcium. *FEBS Lett.* 1999, *462*, 377–382.

[33] Schwacke, R., Schneider, A., van der Graaff, E., Fischer, K. *et al.*, ARAMEMNON, a novel database for Arabidopsis integral membrane proteins. *Plant Physiol.* 2003, *131*, 16–26.

[34] Fuglsang, A. T., Visconti, S., Drumm, K., Jahn, T. *et al.*, Binding of 14-3-3 protein to the plasma membrane $H^+$-ATPase AHA2 involves the three C-terminal residues Tyr946–Thr-Val and requires phosphorylation of Thr947. *J. Biol. Chem.* 1999, *274*, 36774–36780.

[35] Schoonheim, P. J., Veiga, H., Pereira Dda, C., Friso, G. *et al.*, A comprehensive analysis of the 14-3-3 interactome in barley leaves using a complementary proteomics and two-hybrid approach. *Plant Physiol.* 2007, *143*, 670–683.

[36] Aducci, P., Camoni, L., Marra, M., Visconti, S., From cytosol to organelles: 14- 3-3 proteins as multifunctional regulators of plant cell. *IUBMB Life* 2002, *53*, 49–55.

[37] Roberts, M. R., 14-3-3 proteins find new partners in plant cell signaling. *Trends Plant Sci.* 2003, *8*, 218–223.

[38] Kanczewska, J., Marco, S., Vandermeeren, C., Maudoux, O. *et al.*, Activation of the plant plasma membrane $H^+$-ATPase by phosphorylation and binding of 14-3-3 proteins converts a dimer into a hexamer. *Proc. Natl. Acad. Sci. USA* 2005, *102*, 11675–11680.

[39] Duby, G. and Boutry, M., The plant plasma membrane proton pump ATPase: a highly regulated P-type ATPase with multiple physiological roles. *Pflugers Arch.* 2009, *457*, 645–655.

[40] Ryu, H., Kim, K., Cho, H., Park, J. *et al.*, Nucleocytoplasmic shuttling of BZR1 mediated by phosphorylation is essential in Arabidopsis brassinosteroid signaling. *Plant Cell* 2007, *19*, 2749–2762.

 

[41] Gampala, S. S., Kim, T. W., He, J. X., Tang, W. *et al.*, An essential role for 14-3-3 proteins in brassionsteroid signal transduction in Arabidopsis. *Dev. Cell* 2007, *13*, 177–189.

[42] Ache, P., Becker, D., Ivashikina, N., Dietrich, P. *et al.*, GORK, a delayed outward rectifier expressed in guard cells of *Arabidopsis thaliana*, is a $K^+$-selective, $K^+$-sensing ion channel. *FEBS Lett.* 2000, *486*, 93–98.

[43] Hosy, E., Vavasseur, A., Mouline, K., Dreyer, I. *et al.*, The Arabidopsis outward $K^+$ channel GORK is involved in regulation of stomata movements and plant transpiration. *Proc. Natl. Acad. Sci. USA* 2003, *100*, 5549–5554.

[44] vanden Wijngaard, P. W., Sinnige, M. P., Roobeek, I., Reumer, A., *et al.*, Abscisic acid and 14-3-3 proteins control K+channel activity in barley embryonic root. *Plant J.* 2005, *41*, 43–55.

[45] Latz, A., Becker, D., Hekman, M., Muller, T. *et al.*, TPK1, a Ca(2+)-regulated Arabidopsis vacuole two-pore K(+) channel is activated by 14-3-3 proteins. *Plant J.* 2007, *52*, 449–459.

[46] Sottocornola, B., Visconti, S., Orsi, S., Gazzarrini, S. *et al.*, The potassium channel KAT1 is activated by plant and animal 14-3-3 proteins. *J. Biol. Chem.* 2006, *281*, 35735–35741.

[47] Marmagne, A., Vinauger-Douard, M., Monachello, D., de Longevialle, A. F. *et al.*, Two members of the Arabidopsis CLC (chloride channel) family, AtCLCe and AtCLCf, are associated with thylakoid and Golgi membranes, respectively. *J. Exp. Bot.* 2007, *58*, 3385–3393.

[48] Chiu, J. C., Brenner, E. D., DeSalle, R., Nitabach, M. N. *et al.*, Phylogenetic and expression analysis of the glutamate-receptor-like gene family in *Arabidopsis thaliana*. *Mol. Biol. Evol.* 2002, *19*, 1066–1082.

[49] Sanders, D., Pelloux, J., Brownlee, C., Harper, J. F., Calcium at the crossroads of signaling. *Plant Cell* 2002, *14*, S401–S417.

[50] Qi, Z., Stephens, N. R., Spalding, E. P., Calcium entry mediated by GLR3.3, an Arabidopsis glutamate receptor with a broad agonist profile. *Plant Physiol.* 2006, *142*, 963–971.

[51] Kang, S., Kim, H. B., Lee, H., Choi, J. Y. *et al.*, Overexpression in Arabidopsis of a plasma membrane-targeting glutamate receptor from small radish increases glutamate-mediated $Ca^{2+}$ influx and delays fungal infection. *Mol. Cells* 2006, *21*, 418–427.

[52] Guo, H. and Ecker, J. R., The ethylene signaling pathway: new insights. *Curr. Opin. Plant Biol.* 2004, *7*, 40–49.

[53] Alexander, R. D. and Morris, P. C., A proteomic analysis of 14-3-3 binding proteins from developing barley grains. *Proteomics* 2006, *6*, 1886–1896.

[54] Yao, Y., Du, Y., Jiang, L., Liu, J. Y., Interaction between ACC synthase 1 and 14-3-3 proteins in rice: a new insight. *Biochemistry Mosc.* 2007, *72*, 1003–1007.

[55] Wang, K. L., Yoshida, H., Lurin, C., Ecker, J. R., Regulation of ethylene gas biosynthesis by the Arabidopsis ETO1 protein. *Nature* 2004, *428*, 945–950.

[56] Hernandez Sebastia, C., Hardin, S. C., Clouse, S. D., Kieber, J. J., Huber, S. C., Identification of a novel motif for CDPK phosphorylation *in vitro* that suggest ACC synthase may be a CDPK substrate. *Arch. Biochem. Biophys.* 2004, *428*, 81–91.

[57] Igarashi, D., Ishida, S., Fukazawa, J., Takahashi, Y., 14-3-3 proteins regulate intracellular localization of the bZIP transcriptional activator RSG. *Plant Cell* 2001, *13*, 2483–2497.

[58] Eulgem, T., Rushton, P. J., Robatzek, S., Somssich, I. E., The WRKY superfamily of plant transcription factors. *Trends Plant Sci.* 2000, *5*, 199–206.

[59] Robatzek, S. and Somssich, I. E., Targets of AtWRKY16 regulation regulation during plant senescence and pathogen defense. *Genes Dev.* 2002, *16*, 1139–1149.

[60] Xu, X., Chen, C., Fan, B., Chen, Z., Physical and functional interactions between pathogen-induced Arabidopsis WRKY18, WRKY40, and WRKY60 transcription factors. *Plant Cell* 2006, *18*, 1310–1326.

[61] Chollet, R., Vidal, J., O'Leary, M. H., Phosphoenolpyruvate carboxylase: a ubiquitous, highly regulated enzyme in plants. *Annu. Rev. Plant Physiol. Plant Mol. Biol.* 1996, *47*, 273–298.

[62] Wilker, E. W., van Vugt, M. A., Artim, S. A., Huang, P. H. *et al.*, 14-3-3£controls mitotic translation to facilitate cytokinesis. *Nature* 2007, *446*, 329–332.

[63] Chang, I. F., Genomic and proteomic characterization of Arabidopsis cytosolic ribosomes. *PhD dissertation* 2004.

[64] Sang, Y., Zheng, S., Li, W., Huang, B., Wang, X., Regulation of plant water loss by manipulating the expression of phospholipase D{alpha}. *Plant J.* 2001, *28*, 135–144.

[65] Lee, S., Park, J., Lee, Y., Phosphatidic acid induces actin polymerization by activating protein kinases in soybean cells. *Mol. Cells* 2003, *15*, 313–319.

[66] Ohashi, Y., Oka, A., Rodrigues-Pousada, R., Possenti, M. *et al.*, Modulation of phospholipid signaling by GLABRA2 in root-hair pattern formation. *Science* 2003, *300*, 1427–1430.

[67] Potocky, M., Elias, M., Profotova, B., Novotna, Z. *et al.*, Phosphatidic acid produced by phospholipase D is required for tobacco pollen tube growth. *Planta* 2003, *217*, 122–130.

[68] Li, W., Li, M., Zhang, W., Welti, R., Wang, X., The plasma membrane-bound phospholipase D{delta} enhances freezing tolerance in *Arabidopsis thaliana*. *Nat. Biotechnol.* 2004, *22*, 427–433.

[69] Wang, X., Regulatory functions of phospholipase D and phosphatidic acid in plant growth, development, and stress responses. *Plant Physiol.* 2005, *139*, 566–573.

[70] Andoh, T., Kato, T., Jr., , Matsui, Y., Toh-e, A., Phosphoinositide-specific phospholipase C forms a complex with 14-3-3 proteins and is involved in expression of UV resistance in fission yeast. *Mol. Gen. Genet.* 1998, *258*, 139–147.

[71] Testerink, C., Dekker, H. L., Lim, Z. Y., Johns, M. K. *et al.*, Isolation and identification of phosphatidic acid targets from plants. *Plant J.* 2004, *39*, 527–536.

[72] Testerink, C. and Munnik, T., Phosphatidic acid: a multifunctional stress signaling lipid in plants. *Trends Plant Sci.* 2005, *10*, 368–375.

[73] Bargmann, B. O. and Munnik, T., The role of phospholipase D in plant stress responses. *Curr. Opin. Plant Biol.* 2006, *9*, 515–522.

[74] Yan, J., He, C., Wang, J., Mao, Z. *et al.*, Overexpression of the Arabidopsis 14-3-3 protein GF14 lambda in cotton leads to a ''stay green'' phenotype and improves stress tolerance

 

under moderate drought conditions. *Plant Cell Physiol.* 2004, *45*, 1007–1014.

[75] Rienties, I. M., Vink, J., Borst, J. W., Russinova, E., de Vries, S. C., The Arabidopsis SERK1 protein interacts with the AAA-ATPase AtCDC48, the 14-3-3 protein GF14lambda and the PP2C phosphatase KAPP. *Planta* 2005, *221*, 394–405.

[76] Karlova, R., Boeren, S., Russinova, E., Aker, J. *et al.*, The Arabidopsis somatic embryogenesis receptor-like kinase1 protein complex includes brassinosteroid-insensitive1. *Plant Cell* 2006, *18*, 626–638.

[77] Lalle, M., Visconti, S., Marra, M., Camoni, L., *et al.*, ZmMPK6, a novel maize MAP kinase that interacts with 14-3-3 proteins. *Plant Mol. Biol.* 2005, *59*, 713–722.

[78] Roberts, R. L., Mosch, H. U., Fink, G. R., 14-3-3 proteins are essential for RAS/MAPK cascade signaling during pseudohyphal development in *S. cerevisiae*. *Cell* 1997, *89*, 1055–1065.

[79] Fanger, G. R., Widmann, C., Porter, A. C., Sather, S. *et al.*, 14-3-3 proteins interact with specific MEK kinases. *J. Biol. Chem.* 1998, *273*, 3476–3483.

[80] Riedel, J., Tischner, R., Mack, G., The chloroplastic glutamine synthase (GS-2) of tobacco is phosphorylated and associated with 14-3-3 proteins inside the chloroplast. *Planta* 2001, *213*, 396–401.

[81] Bunney, T. D., van Walraven, H. S., de Boer, A. H., 14-3-3 protein is a regulator of the mitochondria and chloroplast ATP synthase. *Proc. Natl. Acad. Sci. USA* 2001, *98*, 4249–4254.

[82] Ito, J., Heazlewood, J. L., Millar, A. H., Analysis of the soluble ATP-binding proteome of plant mitochondria identified new proteins and nucleotide triphosphate interactions within the matrix. *J. Proteome Res.* 2006, *5*, 3459–3469.

 